

## Electronic Supplementary Information

### Cobalt carbonate hydroxide superstructures for oxygen evolution reactions

Simin Zhang, Bing Ni, Haoyi Li, Haifeng Ling, Huihui Zhu, Haiqing Wang and Xun Wang\*

Key Lab of Organic Optoelectronics and Molecular Engineering Department of Chemistry  
Tsinghua University, Beijing 100084, China.

\* Corresponding author's E-mail: [wangxun@mail.tsinghua.edu.cn](mailto:wangxun@mail.tsinghua.edu.cn)

#### Experimental Section

*Chemicals:* Cobalt chloride hydrate ( $\text{CoCl}_2 \cdot 6\text{H}_2\text{O}$ ,  $\geq 98.0\%$ ), urea ( $\geq 99.0\%$ ), sodium glycolate ( $\geq 97.0\%$ ), anhydrous ethanol (73% ~ 75%), KOH ( $\geq 85.0\%$ ) and N-methyl pyrrolidone were all purchased from sinopharm chemical reagent Co., Ltd. Poly(vinylidene fluoride) (PVDF,  $\geq 98.0\%$ ), acetylene black ( $\geq 99.9\%$ ) and carbon paper were purchased from J&K Scientific Ltd.  $\text{IrO}_2$  was purchased from Alfa Aesar Ltd (043396). All of the chemicals are used without further purification.

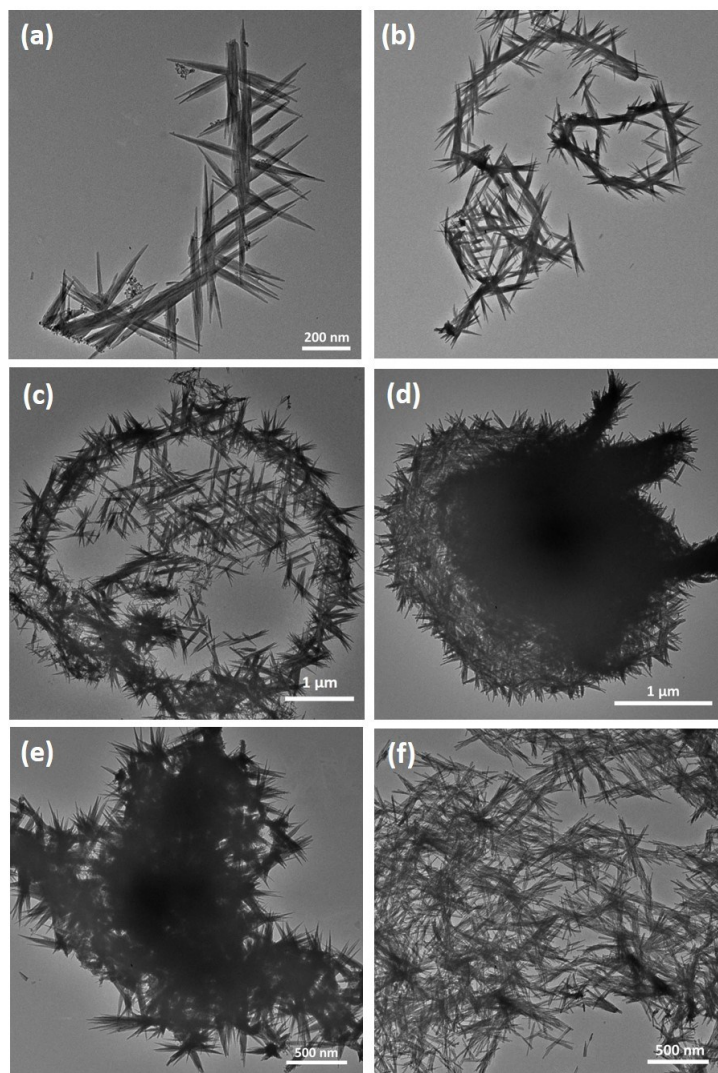
*Preparation of cobalt carbonate hydroxide superstructure:* In a typical procedure, 1.3 mmol  $\text{CoCl}_2 \cdot 6\text{H}_2\text{O}$ , 0.3 mmol urea and 0.2 mmol sodium glycolate were added into 6 mL deionized water and stirred for 10 minutes. Then 2 mL anhydrous ethanol were injected and stirred for another 10 minutes. Finally, the solution was transferred to a 10 mL Teflon-lined stainless steel autoclave and kept at different temperatures for different growth times. After cooling to room temperature, the products were washed with ethanol and deionized water for several times and dried in the air at  $60^\circ\text{C}$  for several hours. In the reaction system, the main reactions might be:



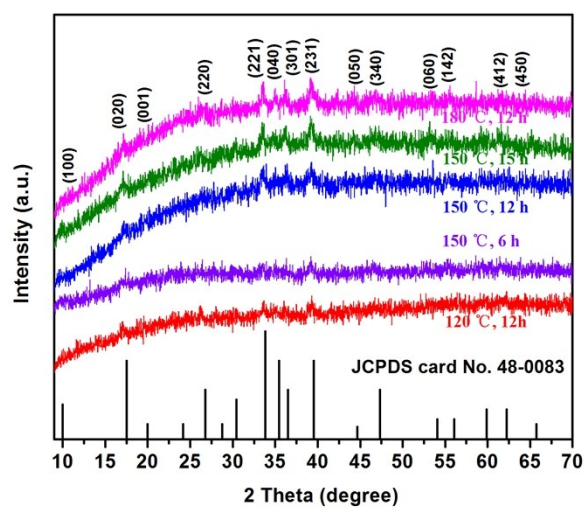
*Characterization:* The structure of the products was characterized by X-ray diffraction (XRD, BrukerD8 Advance,  $\text{Cu K}\alpha$  radiation source) with a scan rate of  $10^\circ \text{min}^{-1}$ . The morphologies of the products were characterized by scanning electron microscope (SEM, HITACHI SU8010), transmission electron microscopy (TEM, HITACHI HT7700) and high-resolution transmission electron microscopy (HRTEM, JEOL JEM 2100F). X-ray photoelectron spectroscopy (XPS) was carried out on PHI Quantera SXM spectrometer (monochromatic  $\text{Al K}\alpha$  and  $\text{Mg/Al}$  dual anode light source). The Fourier transform infrared (FT-IR) spectra was recorded using WQF-510 A FTIR. Thermogravimetric analysis (TGA) was performed on a thermal gravimetric analyzer from room temperature to  $600^\circ\text{C}$  in the air at a heating rate of  $10^\circ\text{C min}^{-1}$ .

*Electrode preparation and Electrochemical measurements:* Carbon papers were cut into  $1 \times 2 \text{ cm}^2$  and ultrasonicated in anhydrous ethanol for 5 min and dried in the air. The test electrodes were prepared by mixing cobalt carbonate hydroxide (75 wt%) with acetylene black (15 wt%) as a conduct agent, polyvinylidene fluoride (PVDF, 10 wt%) dissolved in N-methyl pyrrolidone (NMP) as a binder and grinding carefully. Then this slurry was coated on the treated carbon papers and dried at  $100^\circ\text{C}$  for 12 h under vacuum. The coated area is  $1 \times 1 \text{ cm}^2$  and the mass of active materials is about 2.5 mg on each carbon paper. The electrochemical performance was measured on a Princeton P4000 electrochemistry workstation with a three-

electrode cell using a platinum foil as the counter electrode and an Ag/AgCl electrode as the reference electrode in O<sub>2</sub>-saturated 1 M KOH aqueous electrolyte. Before OER tests, the cyclic voltammetry tests were carried out from 0 V to 0.6 V (vs. Ag/AgCl) at a scan rate of 50 mV s<sup>-1</sup> for ten circles to stabilize and activate the working electrode. The linear sweep voltammetry (LSV) was tested at a scan rate of 1mV s<sup>-1</sup>. The cyclic voltammetry (CV) at different scan rates was measured to determined electrochemical capacitance at 7 different scan rates: 10 mV s<sup>-1</sup>, 40 mV s<sup>-1</sup>, 70 mV s<sup>-1</sup>, 120 mV s<sup>-1</sup>, 160 mV s<sup>-1</sup>, 200 mV s<sup>-1</sup> and 240 mV s<sup>-1</sup> from -0.2 to -0.1 V (vs. Ag/AgCl), which is a 0.1 V potential window centered on the open-circuit potential (OCP). The electrochemical impedance spectroscopy (EIS) was taken at 0.45 V (vs. Ag/AgCl) at a frequency range from 10<sup>5</sup> Hz to 10<sup>-1</sup> Hz.



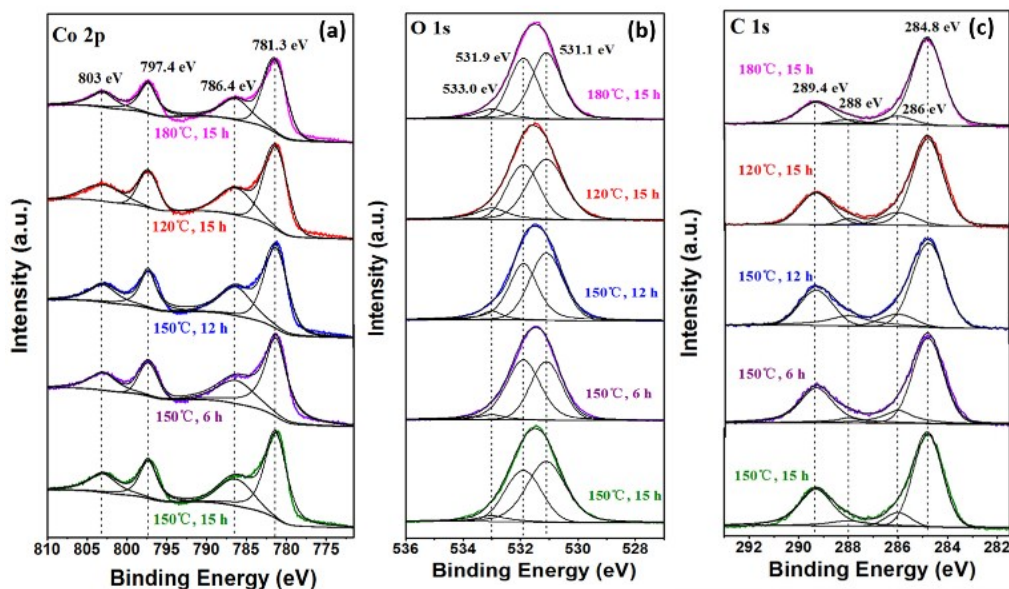
**Figure S1.** TEM images of the products prepared under different hydrothermal conditions: (a) 150°C for 3 h, (b) 150°C for 6 h, (c) 150°C for 9 h, (d) 150°C for 15 h, (e) 120°C for 12 h, (f) 180°C for 12 h.



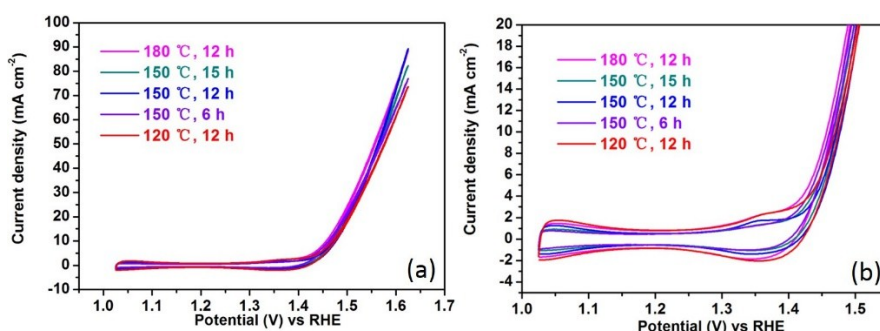
**Figure S2.** XRD patterns of products synthesized under different conditions.

**Table S1.** The elemental analysis results of different samples.

	C (atom ratio)	H (atom ratio)	Co (atom ratio)
150 °C, 12 h	0.465	1.927	0.945
180 °C, 12 h	0.481	1.986	0.952
120 °C, 12 h	0.472	2.132	0.937
150 °C, 6 h	0.464	2.073	0.945
150 °C, 15 h	0.486	2.014	0.959
Cobalt carbonate hydroxide	0.5	1	1

**Figure S3.** High-resolution XPS spectra (d) Co 2p, (e) O 1s, (f) C 1s of products synthesized under different conditions.

As shown in Figure S3., there are two major peaks at 781.3 eV and 797.4 eV are detected in Co 2p core spectrum, which correspond to Co 2p<sub>3/2</sub> and Co 2p<sub>1/2</sub>, respectively. And two shake-up satellite peaks at 786.4 eV and 803 eV are observed. All of these are attributed to the presence of Co<sup>2+</sup>. There are three major peaks at 533 eV, 531.9 eV and 531.1 eV in O 1s core spectrum (Figure S3b.), which correspond to the bonds of oxygen in water, carbonate anions and hydroxyl, respectively. The peaks of C 1s core spectrum (Figure S3c.) appeared at 289.4 eV, 288 eV, 286 eV and 284.8 eV, which can be assigned to the bonds of carbon in carbonate anions, C=O bonds, C–O bonds and C–C bonds, respectively.

**Figure S4.** (a) CV curves and (b) the local enlarged CV curves of the CCHS/CP, CP and products synthesized at different temperatures or for different reaction times loaded on the CP.

**Table S2.** The definite resistant values of different samples

The samples synthesized under different conditions	$R_s$ ( $\Omega$ )	$R_{ct}$ ( $\Omega$ )	CPE ( $S s^{-n}$ )	n	$W(S s^{-0.5})$
180°C, 12h	0.9425	0.2502	0.01433	0.8747	0.8822
120°C, 12h	0.8601	0.3081	0.03459	0.7658	0.825
150°C, 15h	0.8834	0.3385	0.03049	0.8455	1.178
150°C, 12h	0.9406	0.1498	0.02	0.8989	0.7598
150°C, 6h	0.9991	0.3414	0.019	0.7269	1.091

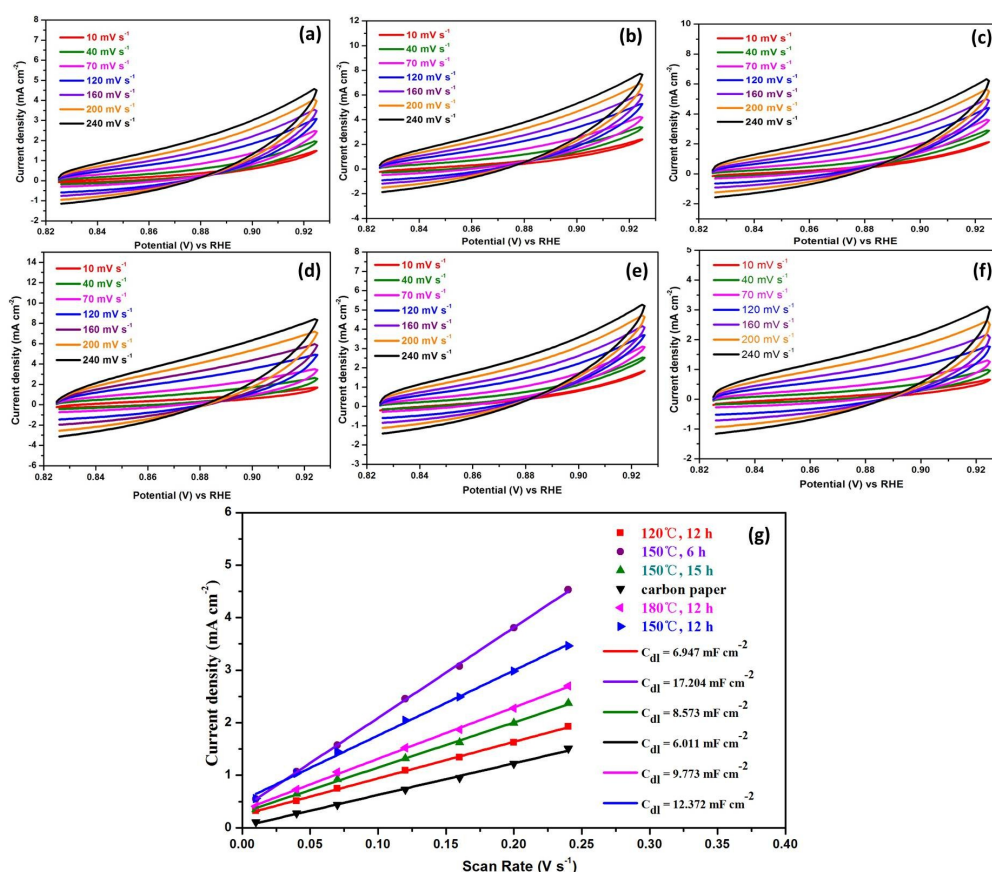


**Figure S5.** Cyclic voltammograms of products synthesized under different conditions: (a) 120°C for 12 h, (b) 150°C for 12 h, (c) 180°C for 12 h, (d) 150°C for 6 h, (e) 150°C for 15 h and (f) carbon paper were measured from -0.2 V to -0.1 V (vs Ag/AgCl). (g) The current density measured at 0.875 V (vs. RHE) plotted as a function of scan rate. The determined double-layer capacitance of the system is consistent with the slope of the linear fits to the data.

**Table S3.** The electrochemical performance of different samples.

Reaction condition	Overpotential for 10 mA cm <sup>-2</sup> / mV	Current density at 1.7 V vs RHE / mA cm <sup>-2</sup>	Tafel slope / mV dec <sup>-1</sup>	$C_{dl}$ / mF cm <sup>-2</sup>
150 °C for 12h	245	162.4	82.06	12.372
180 °C for 12h	245	146.3	84.1	9.773
120 °C for 12h	245	119.6	92.51	6.947
150 °C for 6h	245	133.6	90.39	17.204
150 °C for 15h	240	140	89.48	8.573
carbon paper	465	10.9	118	6.011

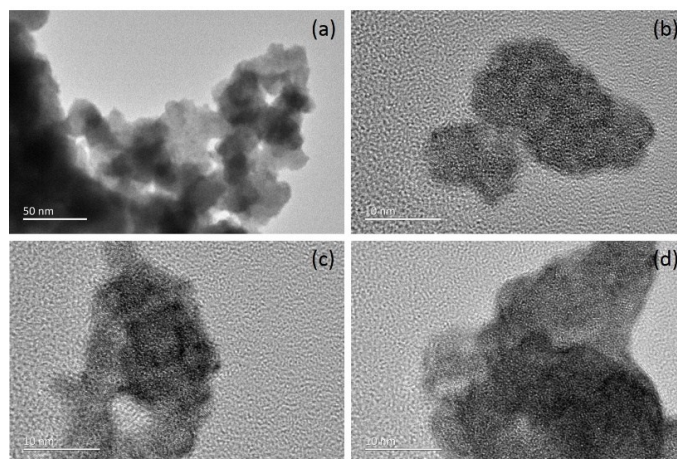


**Figure S6.** (a) (b) (c) (d)HRTEM images of the IrO<sub>2</sub> used in this paper.

The IrO<sub>2</sub> is polycrystalline with irregular particles, and it is not uniform. The particle size ranges from 10 nm to 50 nm or even bigger.

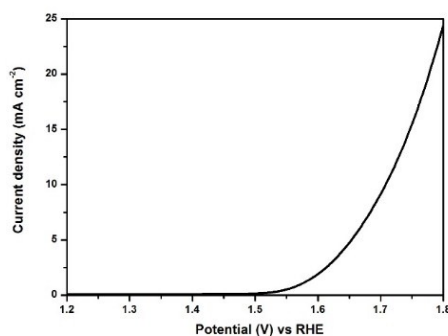


**Figure S7.** The polarization curves of IrO<sub>2</sub> loaded on the rotating disk electrode (RDE) with glassy carbon.

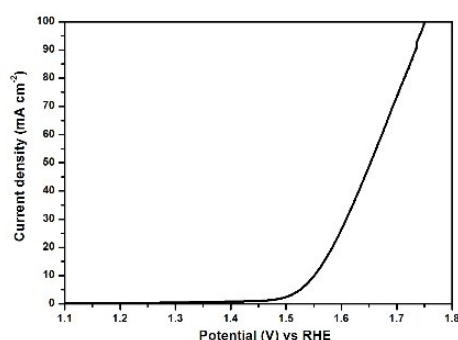


**Figure S8.** The polarization curves of the CCHS loaded on the rotating disk electrode (RDE) with glassy carbon (the loading is 35  $\mu$ g).

**Preparation of samples for OER.** 5 mg of the active material, 1 mg of pure carbon (Vulcan XC72) and 50  $\mu$ L nafion D-521 were added into a mixture solution of 750  $\mu$ L deionized water and 250  $\mu$ L absolute ethanol and then sonicated for 30 min. After that, 7  $\mu$ L of the mixture solution was dropped on a rotating disk electrode, which has 0.196 cm<sup>2</sup> of effective area. After drying naturally, it could be used as the working electrode for tests.

**Table S4.** Comparison of the electrocatalytic oxygen evolution reaction performance of some Co-containing systems.

Materials	Overpotential of 10 mA cm <sup>-2</sup> (mV (vs RHE))	Tafel slope (mV dec <sup>-1</sup> )	The corresponding electrolytes	The sample loading (mg cm <sup>-2</sup> )	Reference
CCHS	320	82.06	1 M KOH	0.178	This work.
Co <sub>3</sub> O <sub>4</sub> nanosheets	330	69	1 M KOH	0.318	<sup>1</sup>
Co <sub>3</sub> O <sub>4</sub> nanoparticles	485	84	1 M KOH	0.2	<sup>2</sup>
LDH FeCo	330	85	1 M KOH	0.21	<sup>3</sup>
Co-based nanoparticles grown on carbon nanosheets	620	266.7	1 M NaOH	0.255	<sup>4</sup>
Ultra-tiny Co(OH) <sub>2</sub> particles supported on graphene oxide	445	N/A	1 M KOH	0.1	<sup>5</sup>
Ultrathin Cobalt–Manganese Layered Double Hydroxide	350	43	1 M KOH	0.142	<sup>6</sup>
porous Fe-doped CoP nanosheet arrays on carbon cloth	342	N/A	1 M KOH	Grown on carbon cloth (very large loading).	<sup>7</sup>
Cobalt carbonate hydroxide supported on carbon	480	N/A	0.1 M KOH	0.18 (Co)	<sup>8</sup>
Nickel-cobalt layered double hydroxide nanosheets	420	113	0.1 M KOH	1.76	<sup>9</sup>

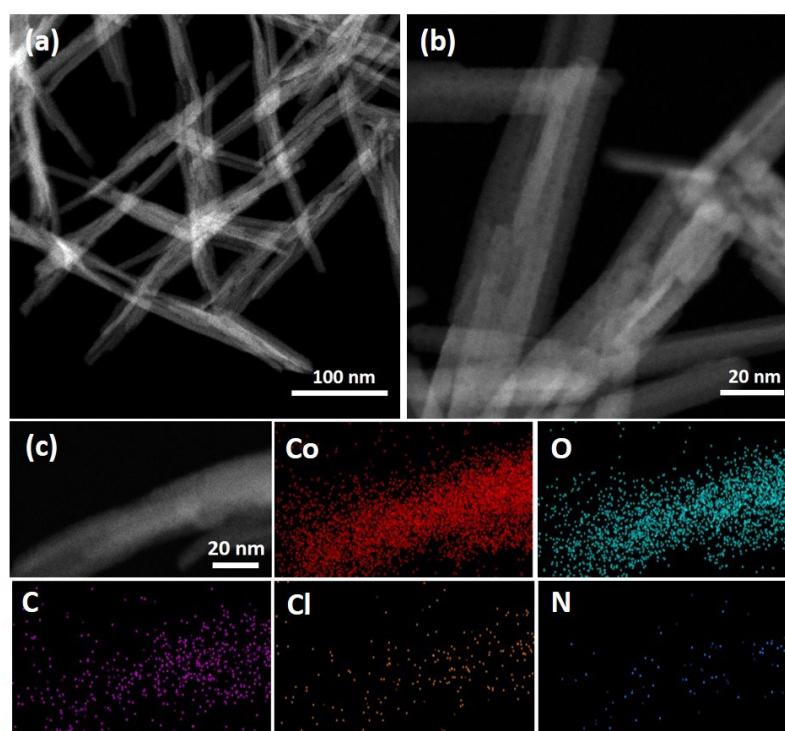


**Figure S9.** (a) (b) STEM images and (c) element mapping of the cobalt carbonate hydroxide 3D superstructure.

As shown in the element mapping, there are a little residue of nitrogen and chlorine in the product, which may belong to the ammonium ions and chloride ions produced by urea and cobalt chloride.

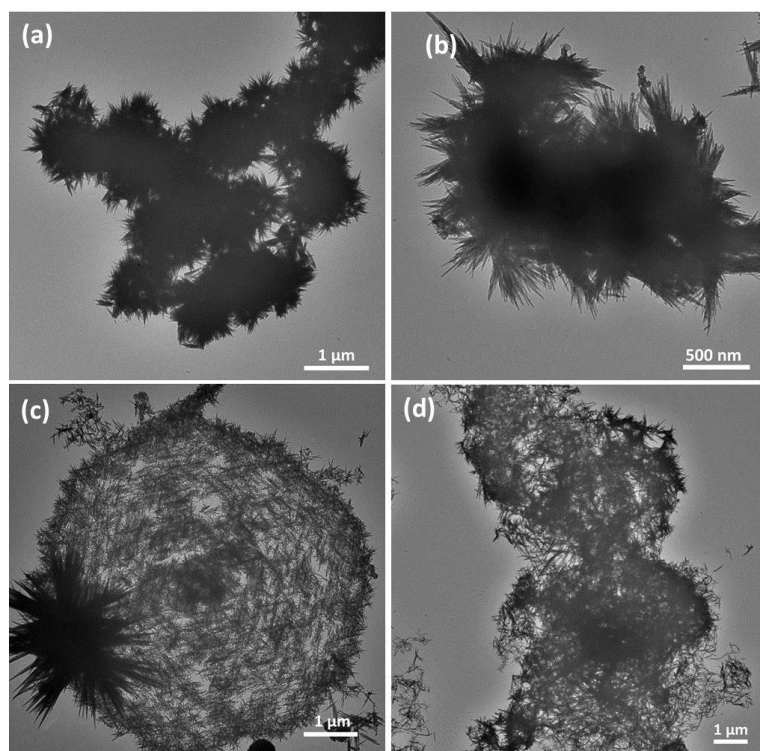


**Figure S10.** TEM images of the products prepared under different hydrothermal conditions: (a) 130°C for 12 h, (b) 130°C for 16 h, (c) 140°C for 12 h, (d) 170°C for 12 h.

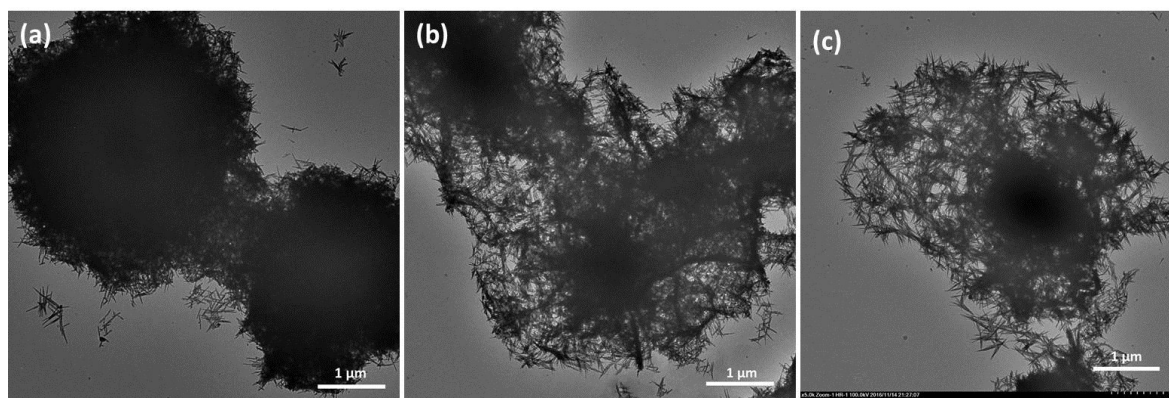


**Figure S11.** TEM images of the products with adding different amounts of sodium glycolate: (a) 0.1 mmol, (b) 0.3 mmol, (c) 0.4 mmol.

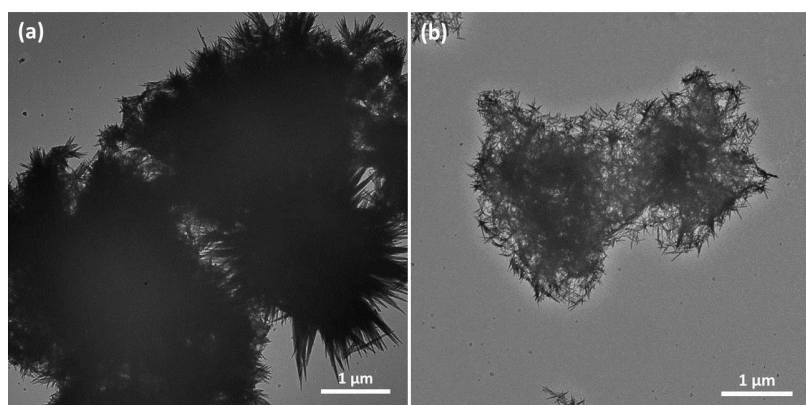


**Figure S12.** TEM images of the products with adding different amounts of urea: (a) 0.2 mmol, (b) 0.5 mmol.

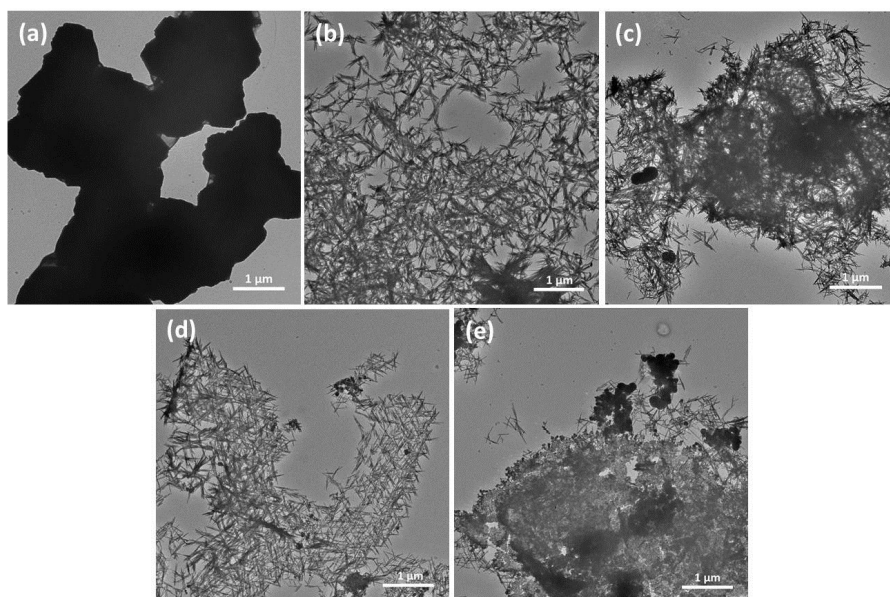


**Figure S13.** TEM images of the products with adding different amounts of water and anhydrous ethanol as the solvent: (a) 8 mL anhydrous ethanol, (b) 4 mL anhydrous ethanol and 4 mL deionized water, (c) 3 mL anhydrous ethanol and 5 mL deionized water, (d) 1 mL anhydrous ethanol and 7 mL deionized water, (e) 8 mL deionized water.

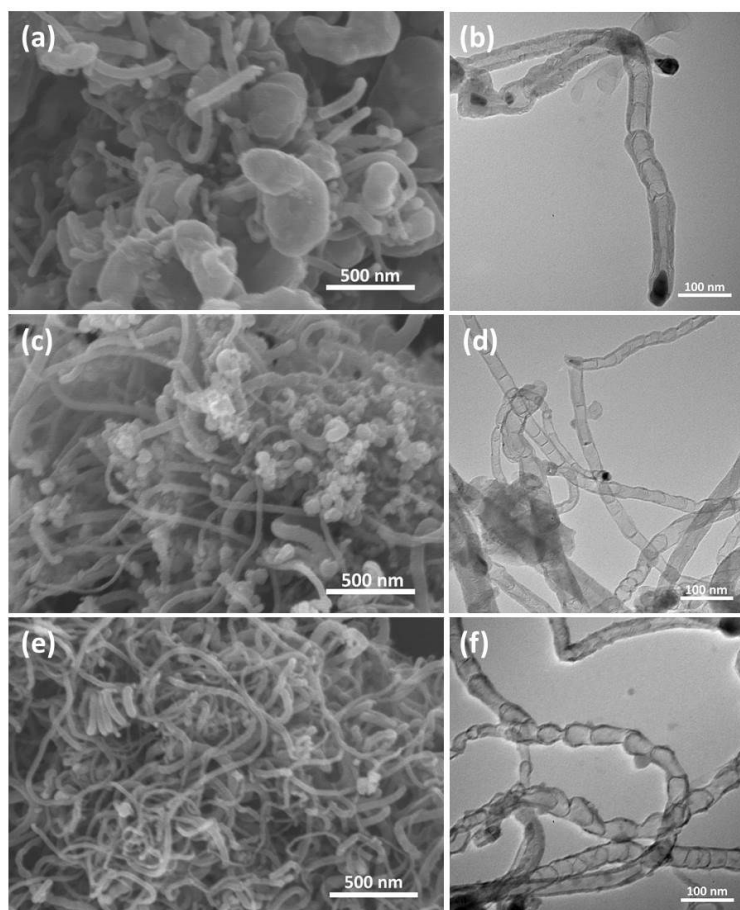


**Figure S14.** SEM images (a), (c), (e) and TEM images (b), (d), (f) of products after calcination. (a) and (b) are for calcined products of pure cobalt carbonate hydroxide superstructure; (c) and (d) are for calcined products of cobalt carbonate hydroxide superstructure with addition of glucose; (e) and (f) are for calcined products of cobalt carbonate hydroxide superstructure with addition of melamine.

30 mg cobalt carbonate hydroxide synthesized at 150°C for 12 h and 3 g glucose or melamine were added into 40 mL deionized water, and then stirred to dry at 80°C. Then the pure cobalt carbonate hydroxide synthesized at 150°C for 12 h, or with addition of glucose or melamine were calcined to 800°C at a rate of 2°C min<sup>-1</sup>.

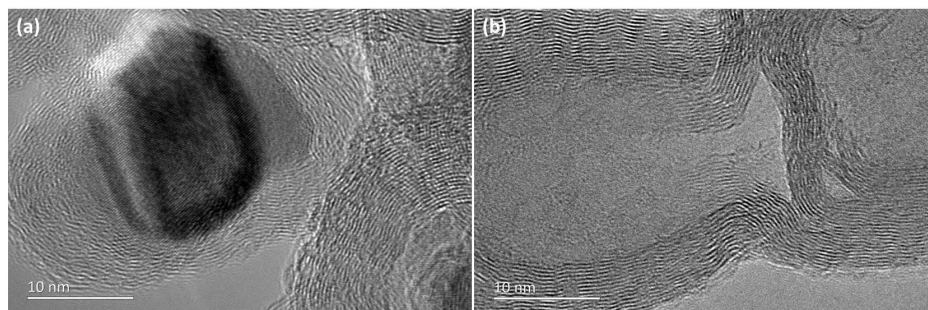


**Figure S15.** HRTEM images of calcined products of cobalt carbonate hydroxide superstructure with addition of melamine.

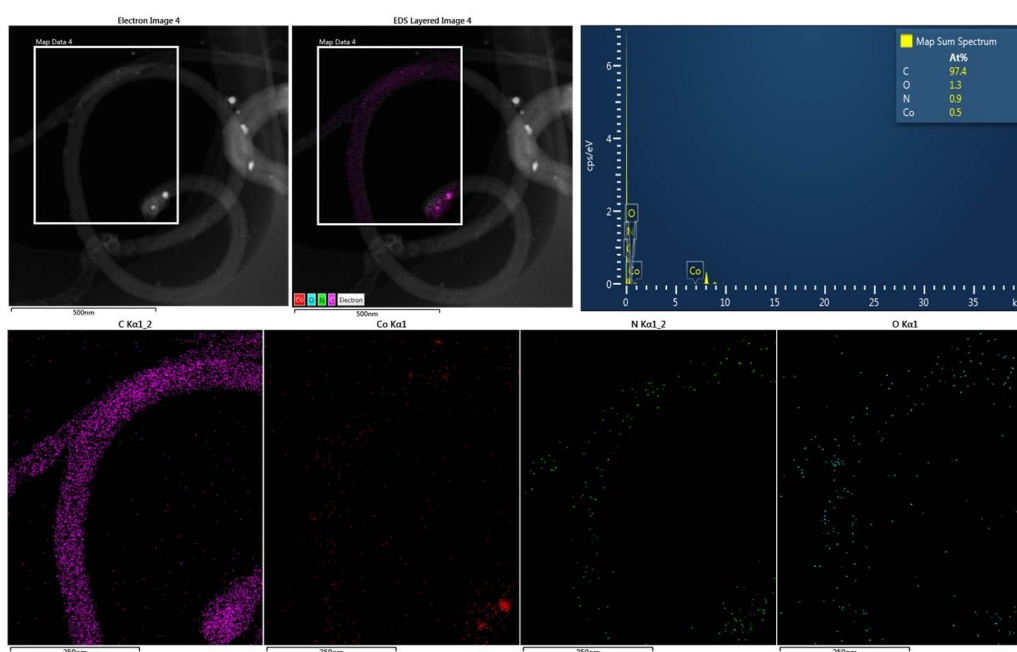


**Figure S16.** The element mapping of calcined products of cobalt carbonate hydroxide superstructure with addition of melamine.

As shown in Figure S14 and S15., the products after calcination is bamboo-like carbon nanotubes, and there are some cobalt at the end of the nanotubes, which might be catalysts. And there are a little nitrogen and oxygen in the products, which can lead to defects.

## Reference

1. S. Du, Z. Ren, Y. Qu, J. Wu, W. Xi, J. Zhu and H. Fu, *Chem. Commun.*, 2016, **52**, 6705-6708.
2. S. Meghdadi, M. Amirasr, M. Zhiani, F. Jallili, M. Jari and M. Kiani, *Electrocatalysis*, 2017, **8**, 122-131.
3. B. Zhang, X. Zheng, O. Voznyy, R. Comin, M. Bajdich, M. García-Melchor, L. Han, J. Xu, M. Liu and L. Zheng, *Science*, 2016, **352**, 333-337.
4. J. Gao, N. Ma, Y. Zheng, J. Zhang, J. Gui, C. Guo, H. An, X. Tan, Z. Yin and D. Ma, *ChemCatChem*, 2017, **9**, 1601-1609.
5. J. Liu, F. Du, H. Zhang, C. Lin, P. Gao, Y. Chen, Z. Shi, X. Li, T. Zhao and Y. Sun, *RSC Advances*, 2015, **5**, 39075-39079.
6. F. Song and X. L. Hu, *J. Am. Chem. Soc.*, 2014, **136**, 16481-16484.
7. S. Hao, L. Yang, D. Liu, R. Kong, G. Du, A. M. Asiri, Y. Yang and X. Sun, *Chem. Commun.*, 2017, **53**, 5710-5713.
8. Y. Wang, W. Ding, S. Chen, Y. Nie, K. Xiong and Z. Wei, *Chem. Commun.*, 2014, **50**, 15529-15532.
9. J. Jiang, A. Zhang, L. Li and L. Ai, *J. Power Sources*, 2015, **278**, 445-451.